BJP BRITISH JOURNAL OF PHARMACOLOGY
BPS BRITISH PHARMACOLOGICAL SOCIETY

British Journal of Pharmacology (2010), 159, 316–325
Journal compilation © 2009 The British Pharmacological Society
No claim to original French government works All rights reserved 0007-1188/09
www.brjpharmacol.org

RESEARCH PAPER

Isolation and pharmacological characterization of AdTx1, a natural peptide displaying specific insurmountable antagonism of the α_{1A}-adrenoceptor

L Quinton[1,2], E Girard[3], A Maiga[4], M Rekik[5], P Lluel[5], G Masuyer[6], M Larregola[7], C Marquer[4], J Ciolek[8], T Magnin[9], R Wagner[9], J Molgó[3], R Thai[4], C Fruchart-Gaillard[4], G Mourier[4], J Chamot-Rooke[1], A Ménez[10]*, S Palea[5], D Servent[4] and N Gilles[4]

[1]*Laboratoire des Mécanismes Réactionnels, Ecole Polytechnique, Palaiseau, France,* [2]*Centre d'Analyse des Résidus en Traces, Université de Liège, Liège, Belgium,* [3]*CNRS, Institut de Neurobiologie Alfred Fessard, Laboratoire de Neurobiologie Cellulaire et Moléculaire, Gif sur Yvette, France,* [4]*CEA, iBiTecS, Service d'Ingénierie Moléculaire des Protéines (SIMOPRO), Gif sur Yvette, France,* [5]*UROsphere S.A.S., Faculté des Sciences Pharmaceutiques, Université Paul Sabatier, Toulouse, France,* [6]*Structural Molecular Biology Department of Biology & Biochemistry, University of Bath, UK,* [7]*UPMC, Laboratoire de Synthèse, Laboratoire des Biomolécules, Paris, France,* [8]*Laboratory of Biophysics, Institute of General and Molecular Biology, N. Copernicus University, Torun, Poland,* [9]*Institut Gilbert-Laustriat UMR 7175 CNRS/Université Strasbourg I, Département Récepteurs et Protéines Membranaires, Ecole Supérieure de Biotechnologie de Strasbourg, Illkirch, France, and* [10]*Muséum national d'Histoire Naturelle, Paris, France*

Background and purpose: Venoms are a rich source of ligands for ion channels, but very little is known about their capacity to modulate G-protein coupled receptor (GPCR) activity. We developed a strategy to identify novel toxins targeting GPCRs.
Experimental approach: We studied the interactions of mamba venom fractions with α_1-adrenoceptors in binding experiments with ^{3}H-prazosin. The active peptide (AdTx1) was sequenced by Edman degradation and mass spectrometry fragmentation. Its synthetic homologue was pharmacologically characterized by binding experiments using cloned receptors and by functional experiments on rabbit isolated prostatic smooth muscle.
Key results: AdTx1, a 65 amino-acid peptide stabilized by four disulphide bridges, belongs to the three-finger-fold peptide family. It has subnanomolar affinity ($K_i = 0.35$ nM) and high specificity for the human α_{1A}-adrenoceptor subtype. We showed high selectivity and affinity ($K_d = 0.6$ nM) of radio-labelled AdTx1 in direct binding experiments and revealed a slow association constant ($k_{on} = 6 \times 10^6 \cdot M^{-1} \cdot min^{-1}$) with an unusually stable α_{1A}-adrenoceptor/AdTx1 complex ($t_{1/2diss} = 3.6$ h). AdTx1 displayed potent insurmountable antagonism of phenylephrine's actions *in vitro* (rabbit isolated prostatic muscle) at concentrations of 10 to 100 nM.
Conclusions and implications: AdTx1 is the most specific and selective peptide inhibitor for the α_{1A}-adrenoceptor identified to date. It displays insurmountable antagonism, acting as a potent relaxant of smooth muscle. Its peptidic nature can be exploited to develop new tools, as a radio-labelled-AdTx1 or a fluoro-labelled-AdTx1. Identification of AdTx1 thus offers new perspectives for developing new drugs for treating benign prostatic hyperplasia.
British Journal of Pharmacology (2010) **159,** 316–325; doi:10.1111/j.1476-5381.2009.00532.x; published online 15 December 2009

Keywords: binding experiments; snake toxin; venom fractionation; mass fragmentation; benign prostatic hyperplasia; iodination; α_{1A}-adrenoceptors

Abbreviations: GPCR, G-protein coupled receptor; NMS, N-methyl-scopolamine; RBS, rat brain synaptosomes

Introduction

G-protein coupled receptors (GPCRs) constitute one of the largest known protein families. They respond to a wide range of structurally diverse chemicals such as biogenic amines, peptides and hormones. They are of considerable clinical importance, serving as targets for about half the drugs in current use. The development of highly selective drugs, with

---

Correspondence: Dr Nicolas Gilles, CEA, Institute of Biology and technologies (iBiTecS), Service d'Ingénierie Moléculaire des Protéines (SIMOPRO), Toxines Récepteur et Canaux, F-91191 Gif sur Yvette, France. E-mail Nicolas.gilles@cea.fr

*This study is dedicated to honour the memory of our colleague Professor André Ménez, who was involved in the original design of this study.

Received 12 March 2009; revised 18 May 2009; accepted 3 August 2009

a known molecular mechanism, is of particular interest, the main objective being to reduce side effects. Most drug development strategies used today are based on chemical modifications of known molecules and virtual screening using a three-dimensional model of the orthosteric binding site (Klebe, 2006). Such strategies, applied to amine-activated GPCRs, which have orthosteric sites located in pockets buried about 11Å below the extracellular surface, predominantly provide low molecular weight organic orthosteric competitors that display either competitive antagonist interactions or direct activation of the target receptor (Bremner *et al.*, 2001; Evers and Klabunde, 2005; Evers *et al.*, 2005). Developing subtype-specific ligands is particularly challenging for receptors with conserved orthosteric binding site sequence and structural organization. We screened animal venoms, representing a natural peptide bank, to identify a novel family of ligands against amine-activated GPCRs. Animal venoms have long been known to contain peptide toxins potently active on ionic channels. Indeed, among the 1800 toxins described in 2006 (King *et al.*, 2008), less than 30 are known to be active on GPCRs.

Toxins active on GPCR are only found in two venomous animals. Marine-cone snails produce toxins acting on vasopressin, neurotensin and adrenoceptors (Nielsen *et al.*, 1994; Craig *et al.*, 1999; Sharpe *et al.*, 2001). Snakes produce sarafotoxins, which are active at endothelin receptors, muscarinic toxins, which act on muscarinic receptors or β-cardiotoxin, which acts on β-adrenoceptors (Bradley, 2000; Ducancel, 2005; Rajagopalan *et al.*, 2007; Servent and Fruchart-Gaillard, 2009). They display a wide variety of pharmacological properties, acting as agonists, antagonists or allosteric modulators (Bradley, 2000; Harvey *et al.*, 2002; Chen *et al.*, 2004; Kukkonen *et al.*, 2004; Birdsall and Lazareno, 2005; Ducancel, 2005; Fruchart-Gaillard *et al.*, 2006). Animal venoms are likely to represent a novel source of new GPCRs ligands.

In this study, we screened mamba snake venom for peptides binding to α_1-adrenoceptors (nomenclature follows Alexander *et al.*, 2008). Adrenoceptors are divided into three classes (α_1, α_2 and β), and α_1-adrenoceptors into three subtypes (α_{1A}, α_{1B} and α_{1D}). α_1-adrenoceptors are involved in the regulation of uro-genital tissue muscle tone (α_{1A} receptors), myocardial contractility (α_{1B} receptors) and vascular tone (α_{1D} receptors, (Koshimizu *et al.*, 2003). Green mamba venom was selected due to its markedly higher potency than other snake venoms and its novel peptide content (le Du *et al.*, 1992; Bradley, 2000; Harvey, 2001). Using a combination of liquid chromatography and binding experiments, we identified AdTx1, the first peptide to show high affinity and selectivity for the human α_{1A}-adrenoceptor subtype. AdTx1 was labelled for use as a pharmacological tool. Functional tests revealed it to be a potent insurmountable antagonist, which was proven to be useful in treating benign prostatic hyperplasia and lower urinary tract symptoms.

Methods

Venom fractionation
One gram of *Dendroaspis angusticep* venom (Latoxan, Valence, France) was separated into 13 fractions (Figure 1) by ion exchange (2 × 15 cm) on Source 15S using a multi-step NaCl gradient at 2 mL·min^{-1} on an Akta purifier (Pfizer, Quebec, Canada). The fraction O was further purified by reverse-phase chromatography (Waters 600) on a preparative column (C18, 15 µm, 20 cm, Vydac, Sigma-Aldrich, Saint Quentin Fallavier, France, 10 mL·min^{-1}), using a linear gradient from 0 to 100% acetonitrile and 0.1% trifluoroacetic acid in 100 min. Analytical high-pressure liquid chromatography (HPLC) was performed on a C18 Vydac column (4.6 mm, 5 µm, 15 cm, 1 mL·min^{-1}) using a gradient of 0.5% acetonitrile min^{-1}.

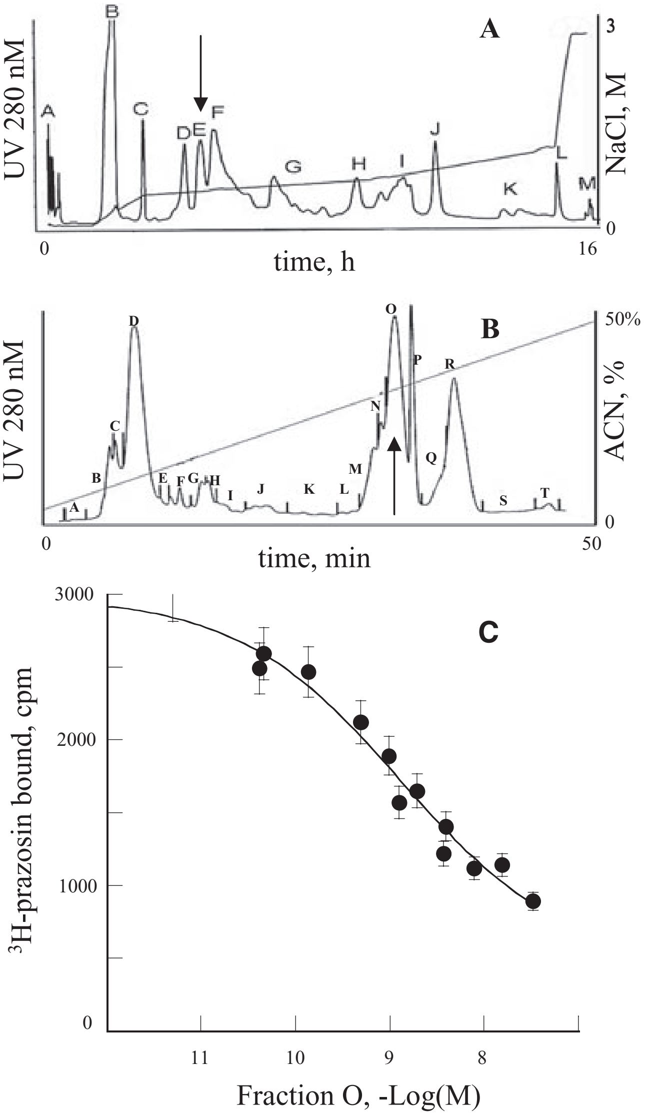

Figure 1 Identification of AdTx1. (A) Ion-exchange chromatography of *Dendroaspis angusticep* crude venom. Labelled peaks were collected (13 fractions). (B) Reverse-phase chromatography of fraction E (arrow) on a Vydac C18 preparative column. Labelled peaks were collected (20 fractions). Fraction O (arrow) was eluted at around 32% acetonitrile (ACN). (C) Inhibition of ^{3}H-prazosin (1 nM) binding by fraction O, quantified using a Bio-Rad protein assay on rat brain synaptosomes (200 µg).

Protein quantification
Fraction O and membrane protein concentrations were determined using the Bio-Rad protein assay, with bovine serum albumin (BSA) as standard.

Mass spectrometry analysis and sequencing
N-terminal sequencing of fraction O (500 pmol loaded on a Biobrene-coated filter) was carried out using Edman chemistry on a Procise Model 492 automatic sequencer from Applied Biosystems (Foster City, CA, USA).

Mass spectrometry was carried out with a 7-T APEX III FT-ICR mass spectrometer (Bruker Daltonics, Bremen, Germany) equipped with a 7 Tesla magnet. A voltage of –700 was applied between the nano-electrospray needles (Proxeon, Odense, Denmark) and the entrance of the glass capillary, for ion transfer at a temperature of 50°C. Mass spectra were acquired from m/z 200 to 3000 with 512 k data points and monoisotopic peaks were labelled using XMASS 6.1.4 software (Bruker Daltonics). For electron capture dissociation experiments, the ion fragment was isolated by radio frequency ejection of all unwanted ions (Cooper *et al.*, 2005). A hollow electron emitter was heated with a 1.9 A current to generate a hollow, tubular electron beam. Isolated multiply charged ions were irradiated for 250 ms with electrons <1 eV kinetic energy. The average of 30 to 50 scans was taken for each spectrum. Fraction O (140 pmol) was reduced and hydrolysed by adding 2.7 pmol of trypsin (E.C3.4.21.4 from bovine pancreas) at 37°C, overnight. Aliquots of 5 pmol were used for peptide mass fingerprinting and 50 pmol was required to obtain electron capture dissociation data.

Synthesis of AdTx1
AdTx1 was synthesized on an Applied biosystems 433A peptide synthesizer (Foster City, CA, USA), purified and folded according to the method described for the muscarinic toxin MT1 (Mourier *et al.*, 2003). Briefly, this involved solid-phase synthesis using a Fmoc strategy, peptide cleavage and purification on a reverse-phase column. The linear peptide was then folded at 4°C for 48 h in the presence of glycerol (25%) and oxidized and reduced glutathione (1 mM) in Tris buffer at pH 8.

AdTx1 iodination
The synthetic AdTx1 was radio-iodinated using 1 nmol of toxin, 0.5 mCi of [^{125}I]-NaI (2200 mCi·mmol^{-1}), 1/50 000 diluted H_2O_2 and 0.7 units of lactoperoxidase (EC 1.11.1.7, Sigma-Aldrich, Saint Quentin Fallavier, France) at pH 7.3, as described (Favreau *et al.*, 2001). The iodinated toxin was purified on reverse-phase chromatography using a C8 chromolite column (VWR, Fontenay sous Bois, France) at a flow rate of 2 mL·min^{-1} and a gradient of 1% acetonitrile per min with 0.1% trifluoroacid (TFA).

Animals. All animal care and experimental procedures were in compliance with French legislation, following the European Council Directive 86/609/EEC regarding the protection of animals used for experimental purposes.

Binding analysis
Rat brain synaptosomes (RBS) were prepared from adult albino Sprague Dawley rats (Favreau *et al.*, 2001). After dissection, the entire brain was homogenized in ice-cold 0.3 M mannitol buffer containing 10 mM EDTA and 10 mM HEPES-Tris, pH 7.4. After centrifugation at 1000× *g* for 10 min, the supernatant was centrifuged at 27 000× *g* for 30 min (P2 pellet). All buffers contained a cocktail of protease inhibitors composed of: phenylmethylsulphonyl fluoride (50 mg·mL^{-1}), pepstatin A (1 mM), iodoacetamide (1 mM) and 1 mM of 1,10-phenanthroline. Membranes from *Pichia pastoris* expressing adrenoceptor subtypes were prepared as described previously after being broken by vigorous vortexing at 4°C for 10 min with 0.5-mm glass beads (Favreau *et al.*, 2001; Andre *et al.*, 2006). Rat heart and lung membranes were prepared using the same methods after processing the corresponding tissues with a Virtis homogenizer. P2 pellets were homogenized at 10 mg·mL^{-1} of protein, frozen in liquid nitrogen and stored at –80°C until used. All binding experiments were performed with 50 mM Tris-HCl, pH 7.4, 10 mM $MgCl_2$ and 1 g·L^{-1} BSA in a final volume of 200 µL. Reaction mixtures were incubated for 24 h (except for the kinetic experiments) at room temperature. Binding reactions were stopped by filtration through a GF/C filter pre-soaked in 0.5% polyethyleneimine. Filters were then washed twice with 2 mL buffer. For tritiated ligands, filters were dried for 1 h at 80°C, mixed with 5 mL of Ultimagold F (PerkinElmer, Courtaboeuf, France) and counted in a Wallac 1211 β-counter (yield of 55%). For iodinated ligands, filters were counted directly in a Wallac 1261 γ-counter (yield of 85%). Non-specific binding was measured in the presence of 1 µM prazosin for ^{3}H-prazosin binding, 1 µM yohimbine for ^{3}H-rauwolscine, 3 µM propanolol for ^{3}H-CGP-12177, 1 µM N-methylscopolamine (NMS) for ^{3}H-NMS or 1 µM AdTx1 for ^{125}I-AdTx1 binding. Inhibition binding data were fitted to either a one-site or two-site/state inhibition mass action curve using Kaleidagraph (Synergy software, Reading, PA, USA). IC_{50} values were converted to K_i for competition experiments using the Cheng-Prusoff equation (Cheng and Prusoff, 1973). Equilibrium saturation experiments were performed with various concentrations of radioactive ligand and a constant quantity of membrane. Kinetic experiments were conducted using a constant amount of radioactive ligand and membrane, with various incubation times. The dissociation kinetics of ^{3}H-prazosin or ^{125}I-AdTx1 were determined after addition of 1 µM of the corresponding cold ligand. The dissociation rate constant (k_{off}) was determined directly from a first order plot of ligand dissociation versus time. The rate of ligand association (k_{on}) was determined from the equation $k_{on} = k_{obs}*([RL]e/([L][RL]max))$, where [L] is the concentration of ligand, [RL]e is the concentration of the complex at equilibrium, [RL]max is the maximum number of receptors present (determined in a parallel saturation experiment) and k_{obs} is determined directly from a first order plot of ligand association versus time. Binding results are presented as mean ± SD (standard deviation) with n, number of independent experiments.

Rabbit isolated prostatic smooth muscle study
The methods used have been described by Delaflotte *et al.* (1996). Briefly, strips of dorsal prostate obtained from albino rabbits were dissected and placed in organ baths containing oxygenated Krebs-Henseleit solution (114 mM NaCl, 4.7 mM

KCl, 2.5 mM $CaCl_2$, 1.2 mM $MgSO_4$, 1.2 mM KH_2PO_4, 25 mM $NaHCO_3$, 11.7 mM glucose, pH 7.4) at 37°C. Propranolol (1 µM), desipramine (0.1 µM), deoxycorticosterone (3 µM) and normetanephrine (1 µM) were added to the Krebs-Henseleit solution in order to block β-adrenoceptors, neuronal and extra neuronal uptake and catechol-O-methyl transferase respectively.

After 60 min of equilibration at the resting tension of 1 g, strips were exposed to 30 µM phenylephrine to test their viability, then 30 min later a first cumulative concentration-response curve to phenylephrine was performed. After a 30 min washout period, strips were incubated with AdTx1 (10, 30 or 100 nM) or its solvent for 180 min and a second concentration-response curve to phenylephrine was performed. Only one concentration for the AdTx1 was tested on each single strip.

Contractile responses were measured with isometric tension transducers (IT-1, EMKA technologies, Paris, France) and recorded using a PowerLab16/s (ADInstruments Pty Ltd, Oxfordshire, UK).

Data analysis. Contractile responses to agonist are presented as mean ± SEM % of maximum tension. Curves were fitted to the one-site mass action equation using GraphPad Prism 4.0 (GraphPad Prism Software Inc., San Diego, CA, USA) for EC_{50} estimation.

For the calculation of AdTx1 antagonist potency, we used the method previously described for insurmountable antagonist producing a clear right-ward displacement of the concentration-response curve to the agonist (Kenakin, 2009).

Briefly, at a level of response, 30% of the control maximal response, an equiactive dose-ratio for agonist concentrations was measured using the concentration-response curve obtained with 30 nM AdTx1. The following equation was used: $pA_2 = -\log[\text{antagonist}] + \log(\text{dose ratio} - 1)$. According to the author (Kenakin, 2009) for low levels of response and for high efficacy agonists, like phenylephrine, the pA_2 will be an accurate estimate of the pK_B.

Materials. Radioactive components were from PerkinElmer. All chemical products and cell culture media were from Sigma-Aldrich. Protected amino-acid derivatives and resins were from Novabiochem (France Biochem, Meudon, France).

Results

Isolation and characterization of AdTx1

Green mamba venom was separated into 13 fractions by cation exchange chromatography (Figure 1A). We investigated the capacity of each fraction to inhibit ^{3}H-prazosin binding to RBS. Fraction E, which significantly reduced ^{3}H-prazosin binding, was sub-fractionated by reverse-phase chromatography (Figure 1B). Pharmacological activity was recovered in peak O, which inhibited ^{3}H-prazosin binding in a concentration-dependent manner, with an IC_{50} in the low nanomolar range and a Hill slope around 0.5 (Figure 1C). Analytical chromatography for fraction O showed a single peak (Figure 2A, line a) and mass analysis revealed a major component, with less than 10% contamination by three other peptides (data not shown). The monoisotopic molecular mass of the major product was 7278.3691 Da before reduction and 7286.3741 Da after reduction, indicating the presence of four disulphide bonds. The sequence of this product was determined by a combination of Edman's degradation (for the first 50 residues) and mass analysis (Table 1). The entire sequence of the peptide product was covered by seven peptides using mass fingerprinting, following reduction and trypsin hydrolysis. The *m/z* 863.37 ($[M + 4H]^{4+}$) ion corresponding to the C-terminal part of the peptide was fragmented by electron capture dissociation (Figure 2B, Cooper *et al.*, 2005). The entire sequence was determined with the exception of three ambiguous amino-acid pairs. The first of these, an AT at position 44–45, was part of the Edman's sequence. The other two pairs were SL/I (54–55) and NE at the C-terminal end. The SI and NE sequences tags were chosen by homology with known sequences (Table 1). The final sequence obtained was:

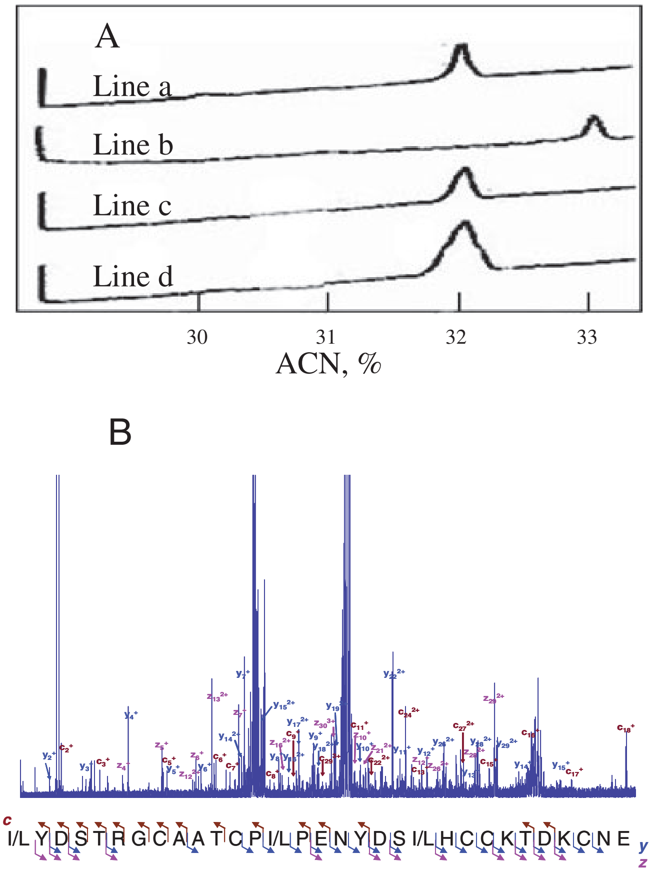

Figure 2 (A) Analytical reverse-phase chromatography of fraction O (line a), reduced AdTx1 (line b) and oxidized AdTx1 (line c). Line d is the co-elution of fraction O and the oxidized synthetic AdTx1. *(B) Identification of the C-terminal part of the sequence of AdTx1. Fragmentation by electron capture dissociation of the *m/z* 863.37 ($[M+4H]^{4+}$) ion obtained after trypsin digestion of fraction O. *c-*, *z-* and *y*-ion types used for the sequencing are indicated in brown, pink and blue respectively.

LTCVTSKSIFGITTEDCPDGQNLCFKRRHYVVPKIYDSTRGCAATCPIPENYDSI-HCCKTDKCNE. The corresponding peptide was chemically synthesized, purified and refolded (Mourier *et al.*, 2003). Comparative analytical HPLC showed that the

Table 1 Sequence alignment of AdTx1. Percentage identities compared with AdTx1 are indicated

		------Edman degradation------	
Edman		LTXVTSKSIFGITTEDXPDGQNLXFKRRHYVVPKIYDSTRGXAATXPIPE	
		---mass sequencing---	
Mass analysis		IYDSTRGCAATCPIPENYDSI-HCCKTDKCNE or IYDSTRGCATACPLPENYDIS-HCCKTDKCEN	
AdTx1	Da	LTCVTSKSIFGITTEDCPDGQNLCFKRRHYVVPKIYDSTRGCAATCPIPENYDSI-HCCKTDKCNE	%
MTβ	Dpp	LTCVTSKSIFGITTEDCPDGQNLCFKRRHYVVPKIYD**I**TRGC**V**ATCPIPENYDSI-HCCKTDKCNE	97
Cm3	Dpp	LTCVTSKSIFGITTEDCPDGQNLCFKRRHYVVPKIYD**I**TRGC**V**ATCPIPENYDSI-HCCKT**E**KCN-	95
MT3	Da	LTCVT**KNT**IFGITTE**N**CP**A**GQNLCFKR**W**HYV**I**P**RYTEI**TRGC**A**ATCPIPENYDSI-HCCKTDKCNE	80
MLT	Nak	LTCV**KE**KSIFG**V**TTEDCPDGQNLCFKR**W**H**MI**VP**GR**Y**KK**TRGCAATCPI**A**EN**R**D**V**I-**E**CC**S**TDKCN-	78
MT4	Da	LTCVTSKSIFGITTE**N**CPDGQNLCFKK**WY**Y**I**VP**RYS**D**I**T**W**GCAATCP**K**P**T**N**VRETIR**CC**E**TDKCNE	75
MT1	Da	LTCVTSKSIFGITTE**N**CPDGQNLCFKK**WY**Y**I**VP**RYS**D**I**T**W**GCAATCP**K**P**T**N**VRETIR**CC**E**TDKCNE	74
MT2	Da	LTCVT**T**KSI**G**G**V**TTEDCP**A**GQN**V**CFKR**W**HYV**T**PK**N**YD**IIK**GCAATCP**KVD**N**N**D**PI-R**CC**G**TDKCN**D**	69
MTα	Dpp	LTCVTSKSIFGITTE**N**CPDGQNLCFK**KWY**Y**LNHRYS**D**I**T**W**GCAATCP**K**P**T**N**VRETI**HCC**E**TDKCNE	69
MT7	Da	LTCV**K**S**N**SI**WFP**T**S**EDCPDGQNLCFKR**WQ**Y**IS**P**RM**YD**F**TRGCAATCP**KA**E**YR**D**V**I-**N**CC**G**TDKCN**K**	68
β-ca.	Oh	**RK**C**LNTPLPLIY**TT--CP**I**GQ**DK**C**V**K**MTIKKL**P**SK**YD**VI**RGC**IDI**CP**KSSADVEV-L**CC**D**T**N**KCN**K**	35

Residues different from AdTx1 are in bold. The two ambiguous amino acid pairs are underlined. Da, *Dendroaspis angusticeps*; Dpp, *Dendroaspis polylepis polylepis*; Nak, *Naja kaouthia*; β-Ca, β-cardiotoxin; Oh, *Ophiophagus hannah*.

synthetic linear peptide (Figure 2A, line b) was more hydrophobic than the folded form (Figure 2A, line c), which was eluted at the same position as the native peptide (Figure 2A, line a). This was confirmed by co-injection (Figure 2A, line d). The oxidized peptide had a monoisotopic mass of 7278.3312 Da, similar to that of the native one. We named this new peptide AdTx1 and we used its synthetic homologue for further studies. The protein sequence data reported in this paper have been deposited in the UniProt database under accession number P85092.

AdTx1 is specific for the α_{1A}AR subtype

Prazosin, rauwolscine, CGP-12177 and NMS are selective orthosteric ligands for α_1-adrenoceptors (prazosin), α_2-adrenoceptors (rauwolscine), β-adrenoceptors (CGP-12177) and muscarinic receptors (NMS). We used RBS as a natural source of α_1 adrenoceptors, α_2 adrenoceptors and muscarinic receptors, and heart and lung membranes as sources of β_1 adrenoceptor and β_2 adrenoceptor respectively (Michelotti *et al*., 2000). Prazosin fully inhibited ^{3}H-prazosin binding to RBS with a Hill coefficient close to 1 (0.9 ± 0.1) and a $K_i = 0.31 \pm 0.06$ nM, $n = 8$ (Figure 3A, Oshita *et al*., 1991). AdTx1 inhibited ^{3}H-prazosin binding, but over a large concentration range, with a Hill coefficient between 0.3 and 0.5, incompatible with the one-site model (data not shown). We applied the mathematical two-site model, which was consistent with a high- ($IC_{50} = 4 \pm 0.5$ nM) and a low- ($IC_{50} = 1500 \pm 450$ nM) affinity site. ^{3}H-rauwolscine binding was inhibited by AdTx1 but at micromolar concentrations only with an estimated IC_{50} of 10 μM (K_i approximately 2.5 μM). Finally, 10 μM AdTx1 was not sufficient to displace ^{3}H-CGP12177 or ^{3}H-NMS from their receptors (Figure 3A).

Prazosin and AdTx1 inhibited ^{3}H-prazosin binding to human-α_{1A}-adrenoceptor on yeast membranes, with IC_{50} values of 1.0 ± 0.1 nM ($K_i = 0.33 \pm 0.04$ nM) and 1.1 ± 0.05 nM ($K_i = 0.35 \pm 0.04$ nM) respectively ($n = 8$, Figure 3B). This experiment also showed that AdTx1 could not totally abolish ^{3}H-prazosin binding to human-α_{1A}-adrenoceptor, as there was a residual binding of 15 ± 5% ($n = 8$). Conversely, AdTx1 had a low affinity for human-$\alpha_{1|B}$-adrenoceptor and rat-α_{1D}adrenoceptor subtypes, with IC_{50} values of 950 ± 110 ($K_i = 317 \pm 37$ nM, $n = 3$) and 1250 ± 250 nM ($K_i = 420 \pm 83$ nM, $n = 3$) respectively (Figure 3B). The high and low affinities of AdTx1 for α_{1A}-adrenoceptor and for α_{1B}adrenoceptors and α_{1D}adrenoceptor, respectively, are in accordance with the two binding sites described on RBS, as these three sub-types are known to be expressed in rat brain (Michelotti *et al*., 2000).

Dissociation kinetic rates for ^{3}H-prazosin were measured in the presence of prazosin (1 μM, $K_{off\ prazosin} = 0.043 \pm 0.015\ min^{-1}$, $n = 4$), in the presence of AdTx1 (1 μM, $K_{off\ AdTx1} = 0.045 \pm 0.011\ min^{-1}$, $n = 3$) or in the presence of both ligands ($K_{off} = 0.044 \pm 0.018$, $n = 3$, Figure 3C).

Direct binding of ^{125}I-AdTx1 to α_{1A}adrenoceptor

To study the direct interaction between AdTx1 and α_{1A}-adrenoceptor, we carried out radio-labelling assays, as previously described (Favreau *et al*., 2001). ^{125}I-AdTx1 had a specific radioactivity of 1870 Ci·mmol^{-1} with a biological activity of 79% (Supplementary Information). The saturation curve using yeast membranes expressing human α_{1A}-adrenoceptor revealed a site displaying mono-exponential saturable binding, with an affinity between 0.6 and 0.9 nM and a B_{max} between 2 and 4 pmol·mg^{-1} protein ($n = 2$, Figure 4A). ^{125}I-AdTx1 binding was fully inhibited by AdTx1 and prazosin with K_i values of 0.6 ± 0.2 nM and 0.37 ± 0.1 nM ($n = 4$, Figure 4B) respectively. ^{125}I-AdTx1 did not display specific binding to human α_{1B}-adrenoceptor, rat α_{1D}adrenoceptor or non-transfected yeast membranes (data not shown). Kinetic analysis revealed slow association ($K_{on} = 6.4 \pm 1.5 \times 10^6 \cdot M^{-1} \cdot min^{-1}$, $n = 2$) and dissociation ($K_{off} = 0.192 \pm 0.003\ h^{-1}$, $n = 6$) kinetics. The resulting affinity of 0.5 nM is consistent with that obtained from equilibrium experiments. ^{125}I-AdTx1 dissociation kinetics determined in the presence of 1 μM prazosin ($K_{off\ prazosin} = 0.198 \pm 0.004\ h^{-1}$, $n = 4$, Figure 4C), was found to be similar to those obtained with AdTx1.

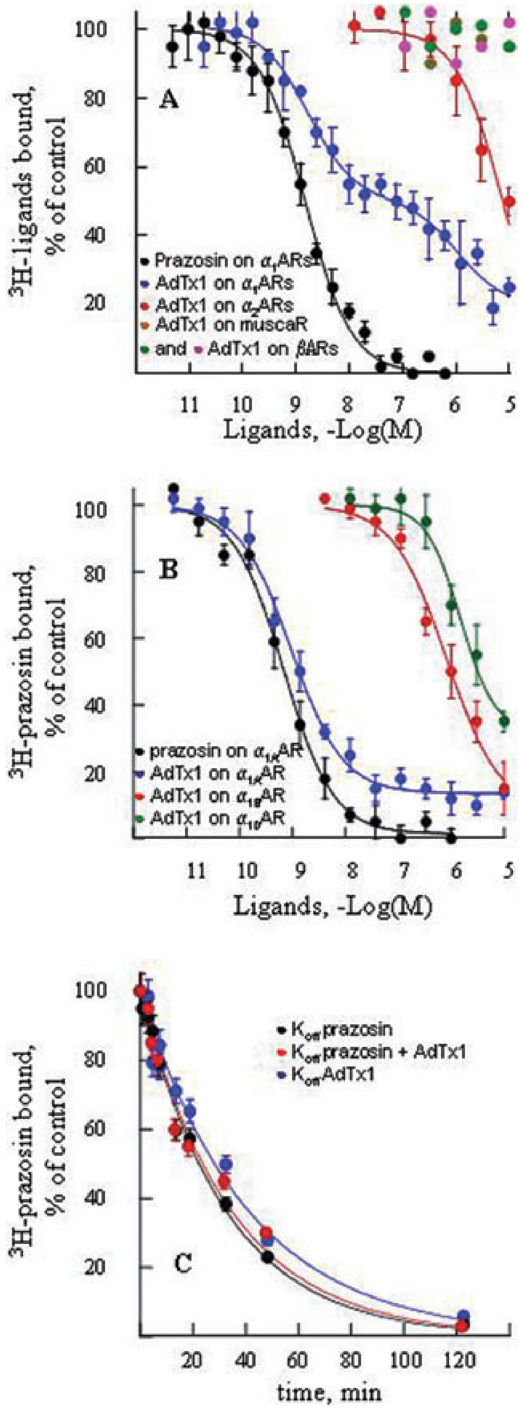

Figure 3 Inhibition binding curves for adrenoceptors and muscarinic receptors. (A) Inhibition curves for natural receptors from different tissues. Curves represent inhibition of ^{3}H-prazosin (1 nM) binding to rat brain synaptosomes (RBS) (200 μg) with various concentrations of prazosin and AdTx1. The inhibition of ^{3}H-rauwolscine (1 nM) binding to RBS (200 μg) by AdTx1 is also shown. Other data represent the non-displacement of ^{3}H-CGP-12177 (1 nM) from heart membranes (100 μg), of ^{3}H-CGP-12177 (1 nM) from lung membranes (100 μg) and of ^{3}H-NMS (0.5 nM) from RBS (100 μg) by AdTx1. (B) Inhibition of ^{3}H-prazosin (1 nM) in yeast membranes (20 μg) expressing human α_{1A}-adrenoceptor with prazosin and AdTx1. There was much weaker inhibition by AdTx1 of ^{3}H-prazosin (1 nM) binding in yeast membranes expressing human-α_{1B}-adrenoceptor (30 μg) or rat α_{1D}-adrenoceptor (50 μg). (C) Kinetic analysis of the dissociation of ^{3}H-prazosin bound to human α_{1A}-adrenoceptor. ^{3}H-prazosin dissociation rate from α_{1A}-adrenoceptor (20 μg), induced by prazosin (1 μM) or AdTx1 (1 μM) or both.

AdTx1 displays insurmountable antagonism in rabbit isolated prostate smooth muscle

The mode of action of AdTx1 was further characterized in functional experiments using smooth muscle isolated from rabbit prostate gland, in which agonist-induced contraction is mediated mainly by activation of α_{1A}-adrenoceptor (Delaflotte *et al*., 1996). Treatment of tissues with solvent had no effect on the second concentration-response curve obtained with phenylephrine; indeed, we observed similar pEC_{50} values for the first (5.22 ± 0.05) and second concentration-response curves obtained (5.28 ± 0.05). Pre-incubation of 10 nM AdTx1 had no effect on cumulative concentration-response curves for phenylephrine. However, AdTx1 concentrations of 30 and 100 nM decreased both phenylephrine potency (pEC_{50} = 4.81 ± 0.14 and 4.27 ± 0.29 respectively) and phenylephrine efficacy, in a concentration-dependent manner. Maximal contractions were 58.8 ± 4.3% (30 nM AdTx1) and 14.0 ± 2.2% (100 nM) (n = 6, Figure 5). Schild plot was not generated due to the great decrease of phenylephrine efficacy. As described in Methods, we calculated a pA_2 of 8.38 in the presence of 30 nM AdTx1.

Discussion

Snakes belonging to the genus *Dendroaspis* (mamba) are extremely dangerous for mammals. Although their venoms are highly toxic, they contain not only very potent neurotoxins, but also several peptides with low or no toxicity (Joubert, 1985). The pharmacological characteristics of most of these non-toxic peptides, identified during the 1970s and 1980s, have not yet been determined. The two peptides sharing the highest level of sequence identity with AdTx1 were MTβ and Cm-3, from the *Dendroaspis polylepis polylepis* venom (Table 1). All the divergent positions between AdTx1 and MT-β and Cm-3 (serine 38, alanine 43, aspartic acid 61 and glutamic acid 63) are located near the knot formed by the disulphide bridges, far from the tip of the fingers, areas which have been identified as important for the pharmacological activities of the three-finger-fold toxins (Servent and Menez, 2001). These observations suggest that the three toxins, AdTx1, MTβ and Cm-3, probably display similar biological activity. MTβ has been shown to exert a very low level of inhibition at muscarinic receptors (Joubert, 1985; Jolkkonen *et al*., 1995; 2001), that is compatible with our results. However, nothing is known about the pharmacological profile of Cm-3, except that this peptide is not toxic. Indeed, whereas 0.1 mg·kg^{-1} of homologous neurotoxin is enough to kill mice by i.v. injection, 50 mg·kg^{-1} of Cm-3 does not induce any visible signs of toxicity (Joubert, 1985). Thus, we can hypothesize that AdTx1 induces also a very low toxicity in mice.

In the green mamba venom used in this study, we identified more than 300 different peptides (unpublished data), of

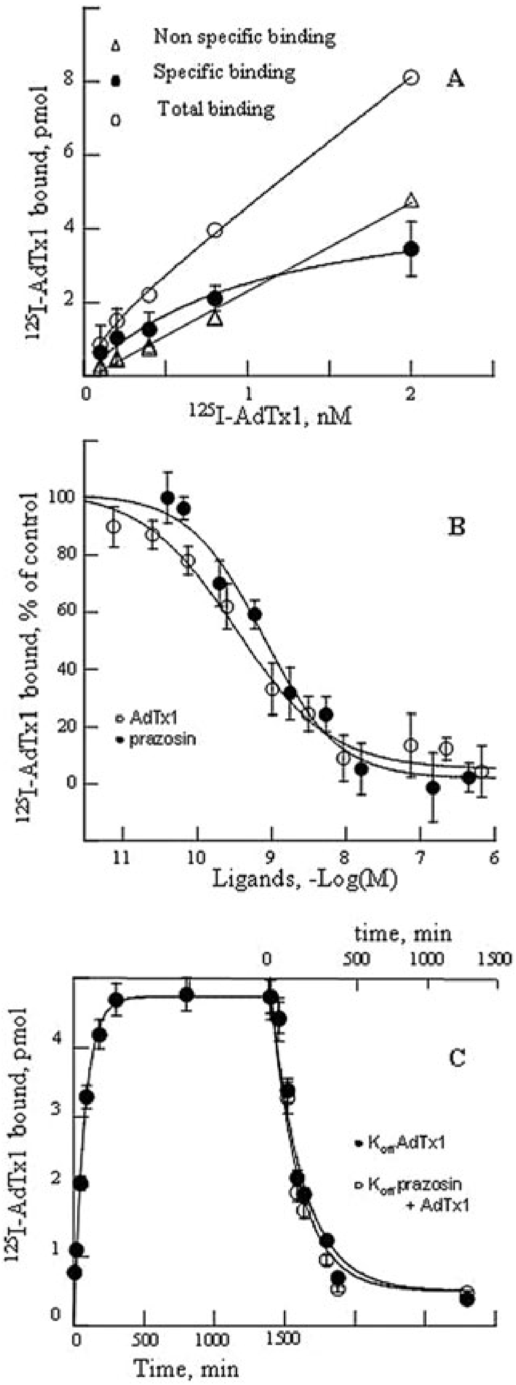

Figure 4 Binding of ^{125}I-AdTx1 to human α_{1A}-adrenoceptor (20 µg). (A) Saturation binding assays for ^{125}IAdTx1 (0.1 to 2 nM) binding to human α_{1A}-adrenoceptor. (B) Displacement of ^{125}I-AdTx1 (0.2 nM) by various concentrations of prazosin and synthetic AdTx1. (C) Association of ^{125}I-AdTx1 (0.2 nM) on human α_{1A}-adrenoceptor. The AdTx1/α_{1A}-adrenoceptor complex is stable for at least 24 h. ^{125}I-AdTx1 (0.2 nM) dissociation, after 16 h of association with human α_{1A}-adrenoceptor, was induced by 1 µM AdTx1 alone or in addition to 1 µM prazosin.

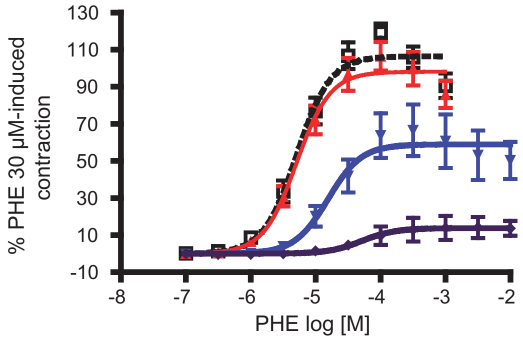

Figure 5 Rabbit isolated prostate muscle. Cumulative concentration-response curves for phenylephrine (PHE) were obtained in prostatic strips after 30 min of incubation with vehicle, or 10 nM, 30 nM or 100 nM AdTx1. Contractile responses to phenylephrine are presented as mean ± SEM % of the maximal tension obtained with 30 µM of phenylephrine, *n* = 6.

which only 30 have been isolated and less than 20 have been characterized pharmacologically. This venom, and probably other mamba venoms, provides a rich source of peptide ligands that target GPCRs, and which remain to be discovered. The study of interactions between GPCRs and natural peptides from snake venoms should lead to the generation of novel compounds that may improve our understanding of receptor properties.

The sequence obtained for AdTx1 resembles that of a three-finger-fold peptide. Most three-finger-fold toxins interact with the cholinergic system, such as nicotinic receptors, muscarinic receptors and acetylcholinesterases (Servent and Menez, 2001). However, toxins from this family also interact with coagulation factors (Banerjee *et al.*, 2005), calcium channels (de Weille *et al.*, 1991), phospholipids (Kumar *et al.*, 1997), integrin receptors (Wu *et al.*, 2006) and β-adrenoceptors (Rajagopalan *et al.*, 2007). A small number of these peptides are active on adrenoceptors. The recently described β-cardiotoxin binds to β_1 and β_2 adrenoceptor subtypes with micromolar affinity (Rajagopalan *et al.*, 2007). Two muscarinic toxins, MT1 and MT2, decrease ^{3}H-prazosin binding to rat vas deferens membranes, with K_i values of 0.23 and 0.88 µM respectively (Harvey *et al.*, 2002). Finally, the conotoxin ρ-TIA, a 19-residue peptide synthesized by the sea snail *Conus tulipa*, has an affinity of 100 nM for α_{1A}-adrenoceptor and α_{1D}-adrenoceptor and 10 nM for α_{1B}-adrenoceptor (Chen *et al.*, 2004). Thus, all the interactions between toxins and the various adrenoceptor subtypes, characterized to date, display a weak affinity and very low selectivity. By contrast, AdTx1 has a subnanomolar affinity for the α_{1A}-adrenoceptor subtype and is 1000 times more potent on this subtype than on other adrenoceptor subtypes. The sequence of AdTx1 is remarkably similar to those of muscarinic toxins (around 70–80% sequence identity), but is not active at muscarinic receptors. On the other hand, AdTx1 and β-cardiotoxin act on the same GPCR family but share only 35% sequence identity.

Findings from binding experiments with ^{3}H-prazosin and ^{125}I-AdTx1 demonstrated that these two ligands compete for binding to human α_{1A}-adrenoceptor. AdTx1 displays a high level of selectivity, with an affinity a thousand times greater for α_{1A}-adrenoceptor than for α_{1B} adrenoceptor and α_{1D} adrenoceptor. AdTx1 and prazosin have the same affinity for α_{1A}-adrenoceptor, but display large differences in their binding kinetics. AdTx1 showed slow association and dissociation rates with a dissociation half-life of 3.6 h, whereas prazosin had a dissociation half-life around 16 min. The explanation of the inability of the AdTx1 to fully inhibit prazosin binding to α_{1A}-adrenoceptor is still under investigation. An allosteric interaction between prazosin and AdTx1 could explain this observation. Nevertheless, none of these ligands affected the dissociation rates of the others and prazosin was able to fully inhibit AdTx1 binding, excluding an allosteric mechanism. A large difference in the kinetic parameters between the radio-tracer and the competitor could also induce perturbations in binding experiment. Thus, due to the slow rate of AdTx1 dissociation, the incubation time was extended to 16 h. However, the residual binding was still observed, whatever the incubation time tested in the range 6–24 h. One possible explanation of the residual binding could be a difference of accessibility of the ligand binding site for the small tracer (prazosin) and a peptide competitor (AdTx1).

These high levels of affinity and selectivity, together with the peptide structure and long half-life of the AdTx1/α_{1A}-adrenoceptor complex, offer novel perspectives for the development of new pharmacological tools. We demonstrated the ability to study direct binding of AdTx1 using iodination, suitable for application to future structure-activity analyses. We also carried out preliminary labelling experiments with fluoro-derivated-AdTx1, using living COS cells that express α_{1A}-adrenoceptor, without requiring fixation or permeabilization of cell (data not shown). Given that no available data describe the precise localization of α_{1A}-adrenoceptor on smooth muscle cells – due mainly to the lack of suitable fluorescent tools – AdTx1 can thus serve as a novel template for developing potent probes.

Isolated prostatic smooth muscle from rabbits was used to evaluate the potential of AdTx1 to relax the smooth muscle. α_1-Adrenoceptor antagonists produce dose-dependent parallel rightward shifts of agonist dose-response curves with no alteration of the maximal response (Tambaro *et al.*, 2005; Muramatsu *et al.*, 2008; Palea *et al.*, 2008). AdTx1 alone acted as an insurmountable antagonist, in that it reduced both the potency and efficacy of phenylephrine. Indeed, 30 nM AdTx1 reduced the maximal response of the prostatic muscle by half and 100 nM AdTx1, by seven-fold. This highest tested concentration of AdTx1 saturated the α_{1A}-adrenoceptor, with almost no binding observed at the two other α_1-adrenoceptor subtypes. The fact that phenylephrine induced only a minor muscle contraction in the presence of AdTx1 at this concentration is consistent with the notion that prostatic muscle tone is mainly mediated by the α_{1A}-adrenoceptor. Two potential mechanisms of action may underlie the insurmountable antagonist effect of AdTx1 (Vauquelin *et al.*, 2002a,b; Kenakin, 2004; Kenakin *et al.*, 2006). AdTx1 could act as a modulator, reducing the affinity for orthosteric ligands, as observed for the toxin MT7, a negative allosteric compound specific to the M1 muscarinic receptor which reduces the potency and efficacy of carbachol-induced increases in Ca^{2+} (Kukkonen *et al.*, 2004). Our binding studies are not consistent with an allosteric binding of AdTx1, as shown by its lack of effect on the ^3H-prazosin dissociation kinetics. Alternatively, the insurmountable antagonist effects of this peptide may be due to the stability of the antagonist-receptor complex. In this scenario, for a defined agonist, potency and efficacy would increase with receptor density (Christopoulos and El-Fakahany, 1999; Vauquelin *et al.*, 2002a,b; Kenakin, 2004). The AdTx1- α_{1A}-adrenoceptor complex displays the longest half-life described so far for adrenoceptors. This could lead to an AdTx1 dose-dependent, long-lasting blockade of α_{1A}-adrenoceptor, reducing receptor density, consequently decreasing pEC_{50} and agonist efficacy.

The reduction of phenylephrine efficacy prevented the generation of a Schild plot. Thus, we calculated a pA_2 for AdTx1 of 8.38 at a concentration of 30 nM. This value is similar to the pA_2 for prazosin (7.9; Hiraoka *et al.*, 1995). There is therefore a discrepancy between the similar pK_i values for prazosin (9.51) and AdTx1 (9.46) and their functional potencies (pA_2 values, 7.9 and 8.38 respectively). Similarly, discrepant results have been frequently described in the last 20 years with prazosin and other α_1-adrenoceptor antagonists leading to the hypothesis for the existence of the so-called α_{1L}-adrenoceptor subtype (Muramatsu *et al.*, 2008). Despite intensive research, the molecular identity of this subtype remained elusive. However, it was recently demonstrated that the α_{1L}-adrenoceptor represents a functional 'phenotype' of the α_{1A}-adrenoceptor gene product and that unidentified cell factors must act in concert to determine this phenotype in each specific tissue (Gray *et al.*, 2008). Moreover, using a new binding technique, the presence of both α_{1L}- and α_{1A}-adrenoceptor was recently shown, in rabbit (Su *et al.*, 2008) and human prostate (Morishima *et al.*, 2007). It will be interesting to determine if AdTx1 is able to distinguish the two phenotypes.

Benign prostatic hyperplasia causes a cluster of urinary symptoms. Its prevalence increases with age (Bullock and Andriole, 2006) and α_{1A}-adrenoceptor antagonists are considered the most effective monotherapy for this disease (American Urological Association practice guidelines). AdTx1, with its high level of selectivity and its nature of insurmountable antagonist, could be a valuable lead in the development of a new drug. At the very least, it will provide an excellent template for the rational design of a new class of therapeutic agents, targeting the α_{1A}-adrenoceptor useful for the treatment of benign prostatic hyperplasia and lower urinary tract symptoms, alone or in combination with other drugs.

Acknowledgements

We are very grateful to Dr S. Lazareno (MRC Technology, London, UK) for valuable discussions. We thank Dr. R. Benmaamar (Institut Gilbert-Laustriat, CNRS, Strasbourg, France) for useful corrections. We thank E. Marcon, C. Estienne, N. Colliot, C. Malosse (Ecole Polytechnique, Palaiseau, France) for technical assistance.

Confocal microscopy studies were performed at the C.N.R.S. campus facility (Plate-forme Imagerie et Biologie Cellulaire) partly supported by the ASTRE program of the Conseil Général de l'Essonne. This work was partially supported by the French National Research Agency (L'Agence nationale de la recherche), programs adrenergicpeptides and gpcrcanotox.

Conflicts of interest

None.

References

Alexander SP, Mathie A, Peters JA (2008). Guide to receptors and channels, 3rd edition. *Br J Pharmacol* **153** (Suppl. 2): S1.

Andre N, Cherouati N, Prual C, Steffan T, Zeder-Lutz G, Magnin T *et al.* (2006). Enhancing functional production of G protein-coupled receptors in Pichia pastoris to levels required for structural studies via a single expression screen. *Protein Sci* **15**: 1115–1126.

Banerjee Y, Mizuguchi J, Iwanaga S, Kini RM (2005). Hemextin AB complex, a unique anticoagulant protein complex from Hemachatus haemachatus (African Ringhals cobra) venom that inhibits clot initiation and factor VIIa activity. *J Biol Chem* **280**: 42601–42611.

Birdsall NJ, Lazareno S (2005). Allosterism at muscarinic receptors: ligands and mechanisms. *Mini Rev Med Chem* **5**: 523–543.

Bradley KN (2000). Muscarinic toxins from the green mamba. *Pharmacol Ther* **85**: 87–109.

Bremner JB, Griffith R, Coban B (2001). Ligand design for alpha(1) adrenoceptors. *Curr Med Chem* **8**: 607–620.

Bullock TL, Andriole, GL Jr (2006). Emerging drug therapies for benign prostatic hyperplasia. *Expert Opin Emerg Drugs* **11**: 111–123.

Chen Z, Rogge G, Hague C, Alewood D, Colless B, Lewis RJ *et al.* (2004). Subtype-selective noncompetitive or competitive inhibition of human alpha1-adrenergic receptors by rho-TIA. *J Biol Chem* **279**: 35326–35333.

Cheng Y, Prusoff WH (1973). Relationship between the inhibition constant (K1) and the concentration of inhibitor which causes 50 per cent inhibition (I50) of an enzymatic reaction. *Biochem Pharmacol* **22**: 3099–3108.

Christopoulos A, El-Fakahany EE (1999). Qualitative and quantitative assessment of relative agonist efficacy. *Biochem Pharmacol* **58**: 735–748.

Cooper HJ, Hakansson K, Marshall AG (2005). The role of electron capture dissociation in biomolecular analysis. *Mass Spectrom Rev* **24**: 201–222.

Craig AG, Norberg T, Griffin D, Hoeger C, Akhtar M, Schmidt K *et al.* (1999). Contulakin-G, an O-glycosylated invertebrate neurotensin. *J Biol Chem* **274**: 13752–13759.

Delaflotte S, Auguet M, Chabrier PE (1996). Pharmacological evidence that different alpha 1 adrenoceptor subtypes mediate contraction in rabbit prostate and hypogastric artery. *Acta Physiol Scand* **158**: 241–251.

le Du MH, Marchot P, Bougis PE, Fontecilla-Camps JC (1992). 1.9-A resolution structure of fasciculin 1, an anti-acetylcholinesterase toxin from green mamba snake venom. *J Biol Chem* **267**: 22122–22130.

Ducancel F (2005). Endothelin-like peptides. *Cell Mol Life Sci* **62**: 2828–2839.

Evers A, Klabunde T (2005). Structure-based drug discovery using GPCR homology modeling: successful virtual screening for antagonists of the alpha1A adrenergic receptor. *J Med Chem* **48**: 1088–1097.

Evers A, Hessler G, Matter H, Klabunde T (2005). Virtual screening of biogenic amine-binding G-protein coupled receptors: comparative evaluation of protein- and ligand-based virtual screening protocols. *J Med Chem* **48**: 5448–5465.

Favreau P, Gilles N, Lamthanh H, Bournaud R, Shimahara T, Bouet F *et al.* (2001). A new omega-conotoxin that targets N-type voltage-sensitive calcium channels with unusual specificity. *Biochemistry* **40**: 14567–14575.

Fruchart-Gaillard C, Mourier G, Marquer C, Menez A, Servent D (2006). Identification of various allosteric interaction sites on M1 muscarinic receptor using 125I-Met35-oxidized muscarinic toxin 7. *Mol Pharmacol* **69**: 1641–1651.

Gray K, Short J, Ventura S (2008). The alpha1A-adrenoceptor gene is required for the alpha1L-adrenoceptor-mediated response in isolated preparations of the mouse prostate. *Br J Pharmacol* **155**: 103–109.

Harvey AL (2001). Twenty years of dendrotoxins. *Toxicon* **39**: 15–26.

Harvey AL, Kornisiuk E, Bradley KN, Cervenansky C, Duran R, Adrover M *et al.* (2002). Effects of muscarinic toxins MT1 and MT2 from green mamba on different muscarinic cholinoceptors. *Neurochem Res* **27**: 1543–1554.

Hiraoka Y, Ohmura T, Sakamoto S, Hayashi H, Muramatsu I (1995). Identification of alpha 1-adrenoceptor subtypes in the rabbit prostate. *J Auton Pharmacol* **15**: 271–278.

Jolkkonen M, Adem A, Hellman U, Wernstedt C, Karlsson E (1995). A snake toxin against muscarinic acetylcholine receptors: amino acid sequence, subtype specificity and effect on guinea-pig ileum. *Toxicon* **33**: 399–410.

Jolkkonen M, Oras A, Toomela T, Karlsson E, Jarv J, Akerman KE (2001). Kinetic evidence for different mechanisms of interaction of black mamba toxins MT alpha and MT beta with muscarinic receptors. *Toxicon* **39**: 377–382.

Joubert FJ (1985). The amino acid sequence of protein CM-3 from Dendroaspis polylepis polylepis (black mamba) venom. *Int J Biochem* **17**: 695–699.

Kenakin T (2009). *A Pharmacology Primer: Theory, Application, and Methods, Vol. 3*. Elsevier Academic Press: London.

Kenakin T (2004). Principles: receptor theory in pharmacology. *Trends Pharmacol Sci* **25**: 186–192.

Kenakin T, Jenkinson S, Watson C (2006). Determining the potency and molecular mechanism of action of insurmountable antagonists. *J Pharmacol Exp Ther* **319**: 710–723.

King GF, Gentz MC, Escoubas P, Nicholson GM (2008). A rational nomenclature for naming peptide toxins from spiders and other venomous animals. *Toxicon* **52**: 264–276.

Klebe G (2006). Virtual ligand screening: strategies, perspectives and limitations. *Drug Discov Today* **11**: 580–594.

Koshimizu TA, Tanoue A, Hirasawa A, Yamauchi J, Tsujimoto G (2003). Recent advances in alpha1-adrenoceptor pharmacology. *Pharmacol Ther* **98**: 235–244.

Kukkonen A, Perakyla M, Akerman KE, Nasman J (2004). Muscarinic toxin 7 selectivity is dictated by extracellular receptor loops. *J Biol Chem* **279**: 50923–50929.

Kumar TK, Jayaraman G, Lee CS, Arunkumar AI, Sivaraman T, Samuel D *et al.* (1997). Snake venom cardiotoxins-structure, dynamics, function and folding. *J Biomol Struct Dyn* **15**: 431–463.

Michelotti GA, Price DT, Schwinn DA (2000). Alpha 1-adrenergic receptor regulation: basic science and clinical implications. *Pharmacol Ther* **88**: 281–309.

Morishima S, Tanaka T, Yamamoto H, Suzuki F, Akino H, Yokoyama O *et al.* (2007). Identification of alpha-1L and alpha-1A adrenoceptors in human prostate by tissue segment binding. *J Urol* **177**: 377–381.

Mourier G, Dutertre S, Fruchart-Gaillard C, Menez A, Servent D (2003). Chemical synthesis of MT1 and MT7 muscarinic toxins: critical role of Arg-34 in their interaction with M1 muscarinic receptor. *Mol Pharmacol* **63**: 26–35.

Muramatsu I, Morishima S, Suzuki F, Yoshiki H, Anisuzzaman AS, Tanaka T *et al.* (2008). Identification of alpha 1L-adrenoceptor in mice and its abolition by alpha 1A-adrenoceptor gene knockout. *Br J Pharmacol* **155**: 1224–1234.

Nielsen DB, Dykert J, Rivier JE, McIntosh JM (1994). Isolation of Lys-conopressin-G from the venom of the worm-hunting snail, Conus imperialis. *Toxicon* **32**: 845–848.

Oshita M, Kigoshi S, Muramatsu I (1991). Three distinct binding sites for [3H]-prazosin in the rat cerebral cortex. *Br J Pharmacol* **104**: 961–965.

Palea S, Chang DF, Rekik M, Regnier A, Lluel P (2008). Comparative effect of alfuzosin and tamsulosin on the contractile response of isolated rabbit prostatic and iris dilator smooth muscles: possible model for intraoperative floppy-iris syndrome. *J Cataract Refract Surg* **34**: 489–496.

Rajagopalan N, Pung YF, Zhu YZ, Wong PT, Kumar PP, Kini RM (2007). Beta-cardiotoxin: a new three-finger toxin from Ophiophagus hannah (king cobra) venom with beta-blocker activity. *Faseb J* **21**: 3685–3695.

Servent D, Menez A (2001). Snake neurotoxins that interact with nicotinic acetylcholine receptors. In: Massaro EJ (ed.). *Handbook of Neurotoxicology*. Humana Press, Inc.: Totowa, NJ, pp. 385–425.

Servent D, Fruchart-Gaillard C (2009). Muscarinic toxins: tools for the study of the pharmacological and functional properties of muscarinic receptors. *J Neurochem* **109**: 1193–1202.

Sharpe IA, Gehrmann J, Loughnan ML, Thomas L, Adams DA, Atkins A *et al.* (2001). Two new classes of conopeptides inhibit the alpha1-adrenoceptor and noradrenaline transporter. *Nat Neurosci* **4**: 902–907.

Su TH, Morishima S, Suzuki F, Yoshiki H, Anisuzzaman AS, Tanaka T *et al.* (2008). Native profiles of alpha(1A)-adrenoceptor phenotypes in rabbit prostate. *Br J Pharmacol* **155**: 906–912.

Tambaro S, Ruiu S, Dessi C, Mongeau R, Marchese G, Pani L (2005). Evaluation of tamsulosin and alfuzosin activity in the rat vas deferens: relevance to ejaculation delays. *J Pharmacol Exp Ther* **312**: 710–717.

Vauquelin G, Van Liefde I, Birzbier BB, Vanderheyden PM (2002a). New insights in insurmountable antagonism. *Fundam Clin Pharmacol* **16**: 263–272.

Vauquelin G, Van Liefde I, Vanderheyden P (2002b). Models and methods for studying insurmountable antagonism. *Trends Pharmacol Sci* **23**: 514–518.

de Weille JR, Schweitz H, Maes P, Tartar A, Lazdunski M (1991). Calciseptine, a peptide isolated from black mamba venom, is a specific blocker of the L-type calcium channel. *Proc Natl Acad Sci USA* **88**: 2437–2440.

Wu PL, Lee SC, Chuang CC, Mori S, Akakura N, Wu WG *et al.* (2006). Non-cytotoxic cobra cardiotoxin A5 binds to alpha(v)beta3 integrin and inhibits bone resorption. Identification of cardiotoxins as non-RGD integrin-binding proteins of the Ly-6 family. *J Biol Chem* **281**: 7937–7945.

Supporting information

Additional Supporting Information may be found in the online version of this article:

Figure S1 Iodination of AdTx1. Panel A: HPLC analysis of the iodinated AdTx1. Panel B: Membrane saturation experiment. 40 fmol of ^{25}I-AdTx1 was mixed with increasing quantities of h-a1AAR. Non-specific binding, in the presence of 1 μM AdTx1 was measured for each quantity of membrane and subtracted. The maximum binding level was evaluated at 30 fmol.

Table S1 Biochemical and pharmacological characterization of ^{25}I-AdTx1. The two peaks obtained after HPLC purification were characterized.